Assessing Climate Change Impacts on Live Fuel Moisture and Wildfire Risk Using a Hydrodynamic Vegetation Model

Wu Ma[1], Lu Zhai[2], Alexandria Pivovaroff[3], Jacquelyn Shuman[4], Polly Buotte[5], Junyan Ding[6], Bradley Christoffersen[7], Ryan Knox[6], Max Moritz[8], Rosie A. Fisher[9], Charles D. Koven[6], Lara Kueppers[10], Chonggang Xu[1],*

[1]*Earth and Environmental Sciences Division, Los Alamos National Laboratory, Los Alamos, NM, United States*

[2]*Department of Natural Resource Ecology and Management, Oklahoma State University, Stillwater, OK, United States*

[3]*Atmospheric Science and Global Change Division, Pacific Northwest National Laboratory, Richland, WA, United States*

[4]*National Center for Atmospheric Research, Climate and Global Dynamics, Terrestrial Sciences Section, Boulder, CO, United States*

[5]*Energy and Resources Group, University of California, Berkeley, CA, United States*

[6]*Climate and Ecosystem Sciences Division, Lawrence Berkeley National Laboratory, CA, United States*

[7]*Department of Biology, University of Texas Rio Grande Valley, Edinburg, TX, United States*

[8]*UC ANR Cooperative Extension, Bren School of Environmental Science & Management, University of California, Santa Barbara, CA, United States*

[9]*Centre Européen de Recherche et de Formation Avancée en Calcul Scientifique, Toulouse, France*

[10]*Energy and Resources Group, University of California, Berkeley, and Lawrence Berkeley National Laboratory, Berkeley, CA, United States*

25   *Corresponding author (Chonggang Xu, cxu@lanl.gov)*

26   **Abstract:** Live fuel moisture content (LFMC) plays a critical role in wildfire dynamics, but little

27   is known about responses of LFMC to multivariate climate change, e.g., warming temperature,

28   CO_2 fertilization and altered precipitation patterns, leading to a limited prediction ability of

29   future wildfire risks. Here, we use a hydrodynamic demographic vegetation model to estimate

30   LFMC dynamics of chaparral shrubs, a dominant vegetation type in fire-prone southern

31   California. We parameterize the model based on observed shrub allometry and hydraulic traits,

32   and evaluate the model's accuracy through comparisons between observed and simulated LFMC

33   of three plant functional types (PFTs) under current climate conditions. Moreover, we estimate

34   the number of days per year of LFMC below 79% (which is a critical threshold for wildfire

35   danger rating of southern California chaparral shrubs) from 1960 to 2099 for each PFT, and

36   compare the number of days below the threshold for medium and high greenhouse gas emission

37   scenarios (RCP4.5 and 8.5). We find that climate change could lead to more days per year (5.2-

38   14.8% increase) with LFMC below 79% between the historical (1960-1999) and future (2080-

39   2099) periods, implying an increase in wildfire danger for chaparral shrubs in southern

40   California. Under the high greenhouse gas emission scenario during the dry season, we find that

41   the future LFMC reductions mainly result from a warming temperature, which leads to 9.1-

42   18.6% reduction in LFMC. Lower precipitation in the spring leads to a 6.3-8.1% reduction in

43   LFMC. The combined impacts of warming and precipitation change on fire season length are

44   equal to the additive impacts of warming and precipitation change individually. Our results show

45   that the CO_2 fertilization will mitigate fire risk by causing a 3.5-4.8% increase in LFMC. Our

46   results suggest that multivariate climate change could cause a significant net reduction in LFMC

47   and thus exacerbate future wildfire danger in chaparral shrub systems.

48   **Keywords:** FATES-HYDRO, chaparral shrubs, plant functional types, southern California, CO_2

49   enrichment, climate change

1. Introduction

51   Historical warming and changes in precipitation have already impacted wildfire at a

52   global scale (e.g. Stocks et al. 1998; Gillett et al. 2004; Westerling et al. 2003, 2006) and it is

53   expected that accelerating future warming will continue to significantly influence global wildfire

54   regimes (e.g. Flannigan et al. 2009; Liu et al. 2010; Moritz et al. 2012). So far, prior studies have

55   mainly focused on impacts of dead fuel moisture, fuel loads, and weather conditions on wildfire.

56   Limited studies have applied proxies of live fuel moisture in global-fire models. For example,

57   dead fuel moisture is found to be related to fire ignition and fire spread potential (or potential

58   area burnt) (Aguado et al. 2007), specific weather conditions such as increased vapor pressure

59   deficit (Williams et al. 2019) can lead to a vast increase in fire activity (Goss et al. 2020), and

60   wildfire fuel loads are projected to increase under climate change (Matthews et al. 2012; Clarke

61   et al. 2016). In global-fire models, studies have used proxies of live fuel moisture (Bistinas et al.

62   2014; Kelley et al. 2019) as well as explicit representation of live fuels (Hantson et al. 2016;

63   Rabin et al. 2017). While previous studies provide great insights into fire risks with changes in

64   climate, dead fuel moisture, fuel loads, and representation of live fuel moisture, there is still

65   limited understanding of how climate change influences live fuel moisture content (LFMC) and

66   the consequent wildfire risks. This is particularly true for the combined impacts of warming

67   temperature, altered precipitation, and increasing CO_2 fertilization (Chuvieco et al. 2004;

68   Pellizzaro 2007; Caccamo et al. 2012a, b; Williams et al. 2019; Goss et al. 2020).

69   A measure of water content within living plant tissue in relation to their dry weight,

70   LFMC has been found to be one of the most critical factors influencing combustion, fire spread,

71 and fire consumption (e.g. Agee et al. 2002; Zarco-Tejada et al. 2003; Bilgili & Saglam 2003;

72 Yebra et al. 2008; Dennison et al. 2008; Anderson & Anderson 2010; Keeley et al. 2011). This is

73 because a low LFMC leads to increased flammability and a higher likelihood of ignition

74 (Dimitrakopoulos & Papaioannou 2001). For instance, LFMC was found to be a significant

75 factor contributing to the occurrence of wildfires in Australia (Plucinski 2003; Nolan et al. 2016;

76 Yebra et al. 2018; Rossa & Fernandes 2018; Pimont et al. 2019), Spain (Chuvieco et al. 2009)

77 and California (Santa Monica Mountains; Dennison et al. 2008; Dennison & Moritz 2009;

78 Pivovaroff et al. 2019). Dennison & Moritz (2009) found strong evidence of a LFMC threshold

79 (79%) for southern California chaparral shrubs, which may determine when large fires can occur

80 in this region.

81   Vegetation moisture content is dependent on both ecophysiological characteristics of the

82 species and environmental conditions, including both climatic variables and soil water

83 availability (Rothermel 1972; Castro et al. 2003; Castro et al. 2003; Pellizzaro 2007; Pivovaroff

84 et al. 2019; Nolan et al. 2020). So far, little is known about the relative importance of different

85 climate variables to future LFMC dynamics. On the one hand, warming could contribute to a

86 higher atmospheric demand and higher evapotranspiration (Rind et al. 1990) and thus lead to a

87 lower LFMC. On the other hand, higher CO_2 concentration will decrease stomatal conductance

88 (Wullschleger et al. 2002) and plant water loss, and thus lead to a higher LFMC. The impacts of

89 CO_2 and warming could be complicated by local changes in precipitation patterns and humidity

90 (Mikkelsen et al. 2008).

91   The sensitivity of LFMC to climate change is likely to be affected by plant hydraulic

92 traits (the plant properties that regulate water transport and storage within plant tissues), which

93 affect plant water regulation (Wu et al. 2020). Variations in hydraulic traits reflect contrasting

94   plant drought adaptation strategies when responding to dry conditions. Two contrasting overall

95   strategies are: 1) water stress avoiders and 2) water stress tolerators (Tobin et al. 1999; Wei et al.

96   2019). The "avoiders" are generally characterized by a more conservative hydraulic strategy

97   under water stress by either closing stomata early, dropping leaves or accessing deep water to

98   avoid more negative water potentials and therefore xylem cavitation. Meanwhile, the "tolerators"

99   typically build xylem and leaves that are more resistant to cavitation so that they can tolerate

100   more negative water potential and continue to conduct photosynthesis under water stress.

101   Therefore, compared with the tolerators, the avoiders normally have a lower sapwood density

102   and higher plant water storage capacity in their tissues to avoid cavitation (Meinzer et al. 2003,

103   2009; Pineda-Garcia et al. 2013). Because the avoiders rely on water storage capacity as one way

104   to avoid cavitation thereby maintaining a relatively high LFMC, and water loss from storage

105   should increase with warming, LFMC could be more sensitive to climate change in avoiders

106   relative to tolerators.

107   While over half of terrestrial landscapes on Earth are considered fire-prone (Krawchuk et

108   al. 2009), Mediterranean-type climate regions are routinely impacted by fire, often on an annual

109   basis. This is partly because Mediterranean climate regions are characterized by winter rains

110   followed by annual dry season, when little to no rainfall occurs for several months. Multiday

111   periods of extreme high temperatures, as well as katabatic hot, dry, and intense winds, often

112   punctuate the annual drought, leading to some of the worst fire weather in the world (Schroeder

113   et al. 1964). This can result in wildfires that are large, high-intensity, and stand-replacing

114   (Keeley 1995; Keeley & Zedler 2009; Balch et al. 2017). Globally, Mediterranean climate

115   regions are characterized by evergreen sclerophyllous-leaved shrublands. The Mediterranean

116   climate region in California is dominated by chaparral, which is adapted to the periodic fire

117   regime in California (Venturas et al. 2016). Previous studies have proposed a variety of

118   relationships between chaparral LFMC and fire danger in southern California (Dennison et al.

119   2008; Dennison & Moritz 2009), but less is known about how climate changes could alter LFMC

120   and fire danger. In chaparral, LFMC is usually high during the winter and spring (wet season)

121   and then gradually declines during the dry season (summer and fall), which leads to a typical fire

122   season approximately six months long in southern California (Pivovaroff et al. 2019). One key

123   risk is that severe drought conditions are becoming exacerbated under climate change, which

124   might lead to the occurrence of larger and higher-intensity fires in chaparral (Dennison et al.

125   2008; Dennison & Moritz 2009).

126   There has been a long history of wildfire modeling, with three types of models: 1) fine-

127   scale fire behavior models (e.g. FIRETEC by Linn et al. 2002); 2) landscape-scale fire

128   disturbance models (e.g. LANDIS-II by Sturtevant et al. 2009); and 3) global-scale fire dynamics

129   models (e.g. Hantson et al. 2016; Rabin et al. 2017; SPITFIRE by Thonicke et al. 2010). While

130   these models focus on simulation at different scales, fire measures of the simulation are mainly

131   calculated from climate and dead fuel moisture and currently lack prediction of LFMC dynamics.

132   One key limitation is that most previous models have not yet considered plant hydrodynamics

133   (Holm et al. 2012; Xu et al. 2013; Seiler et al. 2014), which is integral to LFMC prediction.

134   Recently, there have been important improvements to global dynamic and demographic

135   vegetation models by incorporating plant hydrodynamics (McDowell et al. 2013; Xu et al. 2016;

136   Fisher et al. 2018; Mencuccini et al. 2019). These models have been used to study the interaction

137   between elevated CO_2 and drought (Duursma & Medlyn, 2012), the impact of hydraulic traits on

138   plant drought response (Christofferson et al. 2016), the role of hydraulic diversity in vegetation

139   response to drought (Xu et al. 2016) and hydroclimate change (Powell et al. 2018), and

140   vegetation water stress and root water uptake (Kennedy et al. 2019). While the main purpose of

141   the new hydraulic components is to improve the vegetation response to drought, the fact that

142   hydrodynamic models consider tissue water content as a prognostic variable provides an

143   opportunity to assess the climate impacts on LFMC.

144   The objective of this study is to quantify LFMC dynamics and associated changes in fire

145   season duration for a chaparral ecosystem in southern California under climate change using a

146   vegetation demographic model (that resolves the size and age-since-disturbance structure of

147   plant populations) (Xu et al. 2016; Fisher et al. 2018) that incorporates plant hydraulics. We test

148   one overarching hypothesis: future climate change will decrease LFMC and consequently result

149   in a longer fire season as determined by a critical threshold of LFMC (H_0). Specifically, we test

150   the following four sub-hypotheses: 1) warming has a stronger impact on LFMC than CO_2

151   fertilization (H_1); 2) the reductions in spring and autumn precipitation lead to a longer fire season

152   as determined by LFMC (H_2); 3) the combined impacts of warming and precipitation on fire

153   season length are equal to the additive impacts of warming and precipitation change individually

154   (H_3); and 4) LFMC for plants with more conservative hydraulic strategies ("avoiders") will be

155   more vulnerable to warming (H_4).

156   **2. Materials and Methods**

157   To understand climate change impacts on LFMC for the chaparral ecosystem, we applied

158   the Functionally Assembled Terrestrial Simulator (FATES; Fisher et al. 2015; Massoud et al.

159   2019; Koven et al. 2020) coupled with a hydrodynamic vegetation module (FATES-HYDRO;

160   Christoffersen et al. 2016) in the Santa Monica Mountains in California. We validated the model

161   using the observed LFMC for three chaparral shrub plant functional types (PFTs). Then, we

162   applied FATES-HYDRO to estimate long-term dynamics of leaf water content (LWC) during

163 1960-2099 for each PFT using downscaled Earth System Model (ESM) climate scenarios. We

164 converted simulated leaf water content (LWC) to LFMC within leaves and shoots. Based on the

165 simulated LFMC, we evaluated wildfire danger based on the number of days per year of LFMC

166 below the critical value of 79% from 1960 to 2099 for each PFT under RCP 4.5 and 8.5. Finally,

167 we assessed the relative importance of changes in individual and combined climate variables

168 including CO_2, temperature, precipitation, and tested the corresponding hypotheses.

169 **2.1 Study site**

170   The study site is located at the Stunt Ranch Santa Monica Mountains Reserve, in the

171 Santa Monica Mountains in California, USA (N 34° 05', W 118° 39'). Stunt Ranch is dominated

172 by chaparral vegetation, with an elevation of approximately 350 m, a west-facing slope, and a

173 Mediterranean-type climate. The study site harbors an abundance of fauna, particularly birds and

174 reptiles. The mean annual temperature is 18.1°C. The mean annual precipitation is 478 mm,

175 occurring mostly during the wet season (i.e. November-March) with almost no rainfall during the

176 dry season (i.e. April-October). Stunt Ranch last burned in year 1993. We focused on PFTs

177 representing 11 study species (Fig. 1), including chamise (*Adenostoma fasciculatum* - Af), red

178 shank (*Adenostoma sparsifolium* - As), big berry manzanita (*Arctostaphylos glauca* - Ag), buck

179 brush (*Ceanothus cuneatus* - Cc), greenbark ceanothus (*Ceanothus spinosus* - Cs), mountain

180 mahogany (*Cercocarpus betuloides* - Cb), toyon (*Heteromeles arbutifolia* - Ha), laurel sumac

181 (*Malosma laurina* - Ml), scrub oak (*Quercus berberidifolia* - Qb), hollyleaf redberry (*Rhamnus*

182 *ilicifolia* - Ri), and sugar bush (*Rhus ovata* - Ro). Detailed information about the study site and

183 species characterizations found at Stunt Ranch can be found in Venturas et al. (2016) and

184 Pivovaroff et al. (2019).

185 **2.2 FATES-HYDRO model**

186   FATES is a vegetation demographic model (Fisher et al. 2015), which uses a size-

187   structured group of plants (cohorts) and successional trajectory-based patches based on the

188   ecosystem demography approach (Moorcroft et al. 2001). FATES simulates the demographic

189   process including seed production, seed emergence, growth and mortality (Koven et al. 2020).

190   Because the main purpose is to assess LFMC, we controlled for variation in plant size structure

191   that could arise from plant traits or climate differences between model runs by using a reduced-

192   complexity configuration of the model where growth and mortality are turned off and ecosystem

193   structure is held constant. FATES has to be hosted by a land surface model to simulate the soil

194   hydrology, canopy temperature and transpiration. These host land models include the Exascale

195   Energy Earth System Model (E3SM, Caldwell et al., 2019) land model (ELM) as well as the

196   Community Earth System Model (Fisher et al 2015) and the Norwegian Earth system model

197   (NorESM, Tjiputra et al 2013). In this study, we used the DOE-sponsored ELM as our host land

198   model. The time step of FATES to calculate carbon and water fluxes is 30 minutes and it can

199   downscale the data from 6-hourly climate drivers.

200   A key component of FATES, the plant hydrodynamic model (HYDRO, based on

201   Christoffersen et al. 2016), simulates the water flow from soil through root, stem and leaf to the

202   atmosphere. In this model, water flow is calculated based on water pressure gradients across

203   different plant compartments (leaf, stem, transporting roots, absorbing roots and rhizosphere).

204   Specifically, flow between compartment i and $i + 1$ (Q_i) is given by

$$Q_i = - K_i \Delta h_i, \qquad\qquad (1)$$

205   where K_i is the total conductance (kg MPa^{-1} s^{-1}) at the boundary of compartments i and $i + 1$ and

206   Δh_i is the total water potential difference between the compartments:

$$\Delta h_i = \rho_w g (z_i - z_{i+1}) + (\psi_i - \psi_{i+1}), \tag{2}$$

where z_i is compartment distance above (+) or below (-) the soil surface (m), ρ_w is the density of

water (10^3 kg m^{-3}), g is acceleration due to gravity (9.8 m s^{-2}), and ψ_i is tissue or soil matric

water potential (MPa). K_i is treated here as the product of a maximum boundary conductance

between compartments i and $i + 1$ ($K_{max,i}$), and the fractional maximum hydraulic conductance

of the adjacent compartments (FMC_i or FMC_{i+1}), which is a function of the tissue water content.

A key parameter that controls FMC is the critical water potential (P$_{50}$) that leads to 50% loss of

hydraulic conductivity. The tissue water potential is calculated based on pressure-volume (PV)

theory (Tyree & Hammel, 1972; Tyree & Yang, 1990; Bartlett et al., 2012). For leaves, it is

described by three phases: 1) capillary water phase with full turgor, 2) elastic drainage phase

before reaching turgor loss point; and 3) post-turgor loss phase. For other tissues, it only has

phases 2 and 3. Compared to a non-hydrodynamic model, this formulation allows the simulation

of plant water transport limitation on transpiration. For the non-hydrodynamic version of

FATES, the water limitation factor for transpiration (B$_{tran}$) is calculated based on the soil

moisture potential (Fisher et al. 2015). For the hydrodynamic version, B$_{tran}$ is calculated based on

the leaf water potential (ψ_l) (Christoffersen et al. 2016) as follows,

$$B_{tran} = [1 + (\frac{\psi_l}{P_{50\_gs}})^{a_l}]^{-1} \tag{3}$$

where P_{50_gs} is the leaf water potential that leads to 50% loss of stomatal conductance and a_l is

the shape parameter. Please refer to Christoffersen, et al. 2016 for details of formulations of

FMC for different plant tissues.

2.3 Allometry and trait data for model parameterization

227   FATES-HYDRO has a large number of parameters (>80; see Massoud et al. 2019 for a

228   complete list except for hydraulic parameters). Based on a previous sensitivity analysis study

229   (Massoud et al. 2019), we focused our parameter estimation efforts on the most influential

230   parameters for allometry, leaf and wood traits, and hydraulic traits from observations of 11

231   chaparral shrub species (see Supplementary, Table S2), collected from Jacobsen et al. (2008) and

232   Venturas et al. (2016). For this study, we assumed that the allometry of a shrub is analogous to

233   that of a small tree. However, we did make several important modifications to accommodate the

234   allometry of shrub as their height and crown area relationships to diameter could be different

235   from trees. First, instead of using the diameter at breast height as the basis for allometry to

236   calculate the height, crown area and leaf biomass, we used the basal diameter as the basis for

237   shrubs. Second, in the allometry of trees, the diameter for maximum height (d_1:

238   Fates_allom_dbh_maxheight, Table S1) is the same as the diameter for maximum crown area (d_2:

239   Fates_allom_d2ca_max, Table S1). As our data showed that d_1 and d_2 are different for shrubs,

240   we have modified the codes so that the d_1 and d_2 can be set for different values. It is possible that

241   different branching and path length patterns for stems of chaparral species could impact the

242   hydraulics compared to trees; however, FATES-HYDRO treats all the aboveground xylem as a

243   single pool and thus it should not affect our model simulation results.

244   Based on a hierarchical cluster analysis (Bridges 1966) of allometry and trait data, there

245   are a clear separation among the shrub species. First, the dendrogram is built and every data

246   point finally merges into a single cluster with the height shown on the y-axis. Then we cut the

247   dendrogram in order to create the desired number of clusters determined by a pragmatic choice

248   based on hydraulic traits of eleven chaparral shrub species (Fig. 1). R's rect.hclust function

249   (https://www.rdocumentation.org/packages/stats/versions/3.6.2/topics/rect.hclust) was used to

250   see the clusters on the dendrogram. All parameters of allometry, leaf and wood traits, and

251   hydraulic traits were collected from observations shown in the Table S2 and S3 of the

252   supplementary. According to the principle of model parsimony, we do not want to classify the

253   species into more than 3 PFTs. Meanwhile, we also want to differentiate the fundamental plant

254   growth and water use strategies that will determine plant transpiration rate and the corresponding

255   LFMC. If we choose to classify the species into two PFTs (based on the solid horizontal line in

256   Fig. 1), then we will not be able to differentiate species with aggressive and conservative

257   hydraulic strategies in the second group and not be able to test H4. Therefore, the chaparral shrub

258   species were classified into three PFTs (based on the dotted horizontal line in Fig. 1 and Table

259   S3), that are able to differentiate plant growth and hydraulic strategy. The three PFTs include a

260   low productivity, aggressive drought tolerance hydraulic strategy PFT (PFT-LA) with a relative

261   low $V_{c,max25}$ (the maximum carboxylation rate at 25 ^{o}C) and a very negative P_{50} (the leaf water

262   potential leading to 50% loss of hydraulic conductivity); a medium productivity, conservative

263   drought tolerance hydraulic strategy PFT (PFT-MC) represented by a medium $V_{c,max25}$ and a less

264   negative P_{50}, turgor loss point and water potential at full turgor; and a high productivity,

265   aggressive drought tolerance hydraulic strategy PFT (PFT-HA) with a relatively high $V_{c,max25}$

266   and a very negative P_{50}. The mean of species-level trait data weighted by species abundance at

267   the site were used to parameterize FATES-HYDRO.

268   **2.4 Model initialization**

269   Our model simulation is transient in terms of soil water content, leaf water content,

270   carbon and water fluxes. The forest structure (plant sizes and number density) is fixed and is

271   parameterized based on a vegetation inventory from Venturas et al. (2016). The soil texture and

272   depth information are parameterization based on a national soil survey database

273 (https://websoilsurvey.sc.egov.usda.gov/App/WebSoilSurvey.aspx; Table S1). The soil moisture

274 is initialized with 50% of the saturation and the tissue plant water content is initialized so that it

275 is in equilibrium with the soil water potential. We run the model for 10 years based on 1950-

276 1960 climate so that the simulated soil moisture, leaf water content, carbon and water fluxes are

277 not depending on their initial conditions.

278 **2.5 Live Fuel Moisture Content for model validation**

279 In this study, we used measured LFMC to validate simulated LFMC. FATES-HYDRO

280 does not directly simulate the LFMC. Thus, we estimated the LFMC based on simulated LWC.

281 The LWC in the model is calculated as follows,

282 $$\text{LWC} = \frac{fw - dw}{dw} * 100, \qquad (4)$$

283 where, fw is the fresh weight and dw is the dry weight, which are simulated within FATES-

284 HYDRO. Then, we estimated the LFMC within leaves and shoots (< 6 mm diameter) using the

285 empirical equation derived from shrub LFMC and LWC data including the three regenerative

286 strategies [seeder (S), resprouter (R) and seeder–resprouter (SR)], in summer, autumn and winter

287 from Fig. 4 and 5 in Saura-Mas and Lloret's study (2007) as follows (Fig. S4),

288 $$\text{LFMC} = 31.091 + 0.491\text{LWC}, \qquad (5)$$

289 The climate in Saura-Mas and Lloret's study is Mediterranean (north-east Iberian Peninsula),

290 which is consistent with the climate of our study area. LFMC was measured on our site

291 approximately every three weeks, concurrently with plant water potentials in 2015 and 2016.

292 LFMC measurement details can be found in Pivovaroff et al. (2019). For comparison with our

293 model outputs, we calculated the mean LFMC within leaves and shoots for each PFT weighted

294 by the species abundance (Venturas et al. 2016). Species abundance was calculated by dividing

295 mean density of a specific species by the mean density of all species.

296 **2.6 Climate drivers**

297   We forced the FATES-HYDRO model with 6-hourly temperature, precipitation,

298 downward solar radiation, and wind components. Historical climate data during 2012-2019,

299 which were used for FATES-HYDRO calibration, were extracted from a local weather station

300 (https://stuntranch.ucnrs.org/weather-date/). Historical and future climate data during 1950-2099,

301 which were used for simulations of LFMC by FATES-HYDRO model, were downloaded from

302 the Multivariate Adaptive Constructed Analogs (MACA) datasets (Abatzoglou & Brown 2012;

303 http://maca.northwestknowledge.net). The MACA datasets (1/24-degree or approximately 4-km;

304 Abatzoglou & Brown 2012) include 20 ESMs with historical forcings during 1950-2005 and

305 future Representative Concentration Pathways (RCPs) RCP 4.5 and RCP8.5 scenarios during

306 2006-2099 from the native resolution of the ESMs. The gridded surface meteorological dataset

307 METDATA (Abatzoglou, 2013) were used with high spatial resolution (1/24-degree) and daily

308 timescales for near-surface minimum/maximum temperature, precipitation, downward solar

309 radiation, and wind components. Then we downscaled the MACA daily data to 6-hourly based

310 on the temporal anomaly of the observed mean daily data to the hourly data for each day during

311 2012-2019. The model is driven by yearly CO_2 data obtained from Meinshausen et al (2011).

312 **2.7 Hypothesis testing**

313   To test H_0 (future climate change will decrease LFMC and consequently result in a longer

314 fire season as determined by a critical threshold of LFMC), we compared the simulated mean

315 LFMC, derived from modeled leaf water content, under the climate projections from 20 ESMs

316 under RCP 4.5 and 8.5. We then tested if the LFMC during the April-October dry season in the

317 historic period of 1960-1999 is significantly higher than that in the future period of 2080-2099.

318 For the fire season duration, we estimated the number of days per year below a critical threshold

319 of LFMC (79%). Similarly, we tested if the number of days per year below the critical threshold

320 of LFMC during the historical period are significantly different from that during the future

321 period. We used a bootstrapped approach (Jackson 1993) to test if the mean of LFMC or fire

322 season duration are significantly different between these two periods. Specifically, we randomly

323 draw 10000 samples from the simulated residuals of LFMCs or fire season durations estimated

324 by 20 ESMs for these two periods under the null hypothesis that there is no difference in the

325 mean. We then calculated p-values by comparing the simulated mean difference to the empirical

326 distribution of difference estimated from these 10000 samples. See Supplementary section 5.2

327 within Xu et al. (2019) for the details.

328   To test H_1 (warming has a stronger impact on LFMC than CO_2 fertilization), we

329 compared mean simulated LFMC and fire season length for three PFTs with/without CO_2

330 changes (fixed CO_2 at 367 ppm vs dynamic CO_2 concentrations from RCP 4.5 or RCP 8.5) and

331 warming. To remove the future warming trend, future temperature was replaced with historical

332 (1986-2005) temperature data for every 20 year period. Similarly, to test H_2 (the reductions in

333 spring and autumn precipitation lead to a longer fire season as determined by LFMC), we

334 compared the model outputs of LFMC and fire season length for three PFTs with/without

335 precipitation changes. To test H_3 (the combined impacts of warming and precipitation on fire

336 season length are equal to the additive impacts of warming and precipitation change

337 individually), we compared model outputs of LFMC and fire season length for three PFTs under

338 three scenarios: 1) without warming; 2) without precipitation changes; and 3) without warming

339 and precipitation changes. Finally, to test H4 (LFMC for plants with more conservative hydraulic

340 strategies will be more vulnerable to warming), we compared model outputs of LFMC and fire

341 season length across the three different PFTs with different hydraulic strategies.

342 **3. Results**

343 **3.1 Comparison between simulated and measured LFMC**

344   Our results showed that FATES-HYDRO was able to capture variation in the LFMC for

345 different PFTs and soil water content in 5-cm depth (Fig. 2 and S3), also for Chamise in 2018

346 (Fig. S5) although we had limited observed LFMC data. Specifically, the model was able to

347 capture 96%, 86%, and 80% of the variance in observed LFMC for the period of 2015-2016 for

348 three PFTs, respectively (Fig. 2 b, d, f). The model was also able to capture the seasonal

349 dynamics of soil water content, LFMC, and LFMC below the threshold 79% in comparison to

350 observed data (Fig. 2 a, c, e and S3). To validate that FATES-HYDRO is able to capture the

351 interannual variability of LFMC, we compared the simulated LFMC for PFT-LA with the long-

352 term observations of LFMC for the chamise species (*Adenostoma fasiculatum*; Fig. S5). Our

353 results showed that the model is able to reasonably capture the seasonal and interannual

354 variability for the period of 2006-2019 (R^2=0.7), although it underestimates peaks in LFMC in 4

355 of 14 years.

356 **3.2 Changes in the LFMC and fire season length from historical to future periods**

357   Using the validated model driven by climate projections from 20 ESMs under greenhouse

358 gas emission scenarios RCP4.5 and RCP 8.5, we found that the daily mean LFMC during the

359 future period of 2080-2099 was projected to become significantly lower than that during the

360 historical period of 1960-1999 for all three PFTs (Fig 3, P<0.000001). Our results also showed

361 that the spread among models increase with time, suggesting a larger uncertainty in the

362 projection into the future. Specifically, the histogram of daily mean LFMC during the April-

363 October dry season showed that there was a higher probability of low LFMC under future

364 climate conditions (Fig. S1). The daily mean LFMC decreased from 84.7%, 101.3%, and 78.4%

365 during the historical period of 1960-1999 to 81.0-82.8%, 96.3-98.8%, and 74.8-76.6% during the

366 future period of 2080-2099 under both climate scenarios for PFT-LA, PFT-MC, PFT-HA,

367 respectively (Fig 3).

368   Based on the projected LFMC, there was a significant increase in the fire season length

369 with the critical threshold of LFMC from the historical period of 1960-1999 to the future period

370 of 2080-2099 for three PFTs. With the critical threshold of 79% LFMC, the fire season length

371 was projected to increase by 20, 22, 19 days under RCP 8.5 (Fig. 4 and Table S4), and to

372 increase by 9, 11, 8 days under RCP 4.5 (Fig. 4 and Table S4). Our results also showed that the

373 spread among models increase with time, suggesting a larger uncertainty in the projection into

374 the future. The above results for mean LFMC and fire season length support hypothesis H_0 that

375 future climate change will decrease LFMC and consequently result in a longer fire season, as

376 determined by critical thresholds for LFMC, for all three PFTs.

377 **3.3 Relative effects of individual climate changes on the length of the fire season**

378   In order to better understand the relative contribution to fire season length of different

379 climate variables, we ran FATES-HYDRO for three PFTs using meteorological forcings that

380 isolated and removed changes in individual specific variables. Our results showed that the

381 increase in fire season length mainly resulted from warming, which led to 16-23 days (9.1-

382 18.6%) per year increase in fire season length for the critical threshold of 79% LFMC under RCP

383 8.5 (Fig. 5). This is because warming is pushing Vapor Pressure Deficit (VPD) higher, resulting

384   in increased fire season length. For RCP 4.5, the warming contributed to 5-6 days (3.8-4.3%) per

385   year increase in fire season length (Fig. 5). We also found that elevated CO_2 concentrations

386   decreased fire season length with 6-7 days (3.5-4.8%) per year decrease in fire season length

387   under RCP 8.5 (Fig. 5). Under RCP 4.5, CO_2 increases led to 2-3 days (1.5-2.2%) per year

388   decrease in fire season length (Fig. 5). Because the impact of warming on fire season length was

389   stronger than the mitigation from CO_2 enrichment, our results support hypothesis H_1 (warming

390   has a stronger impact on LFMC than CO_2 fertilization).

391   Even though total precipitation was projected to increase in the future, lower precipitation

392   in the spring and autumn (Fig. S2 a, b) led to 8-10 days (6.3-8.1%) per year increase in fire

393   season length with the critical threshold of 79% LFMC under RCP 8.5 (Fig. 5). Under RCP 4.5,

394   the precipitation changes contributed to 1-3 days (0.8-1.6%) increase in fire season length (Fig.

395   5). This result supported hypothesis H_2 that the reductions in spring and autumn precipitation

396   lead to a longer fire season as determined by LFMC.

397   Our results showed that the combined impacts of warming and precipitation on fire

398   season length were equal to the additive impacts of warming and precipitation change

399   individually. This supported hypothesis H_3. Specifically, the combined changes in temperature

400   and precipitation caused 24-33 days per year (15.6-26.8%) increase in fire season length with the

401   critical threshold of 79% LFMC under RCP 8.5 (Fig. 5). Under RCP 4.5, the combined changes

402   in temperature and precipitation caused a 6-9 days per year (4.8-6.1%) change in fire season

403   length.

404   **3.4 Comparison of changes in fire season length among three PFTs under climate change**

405   Regarding three PFTs under both climate scenarios, fire season length of PFT-HA was

406   the longest (167-176 days per year), while fire season length of PFT-MC was the shortest (114-

407   124 per year) during 2080-2099 (Fig. 4). However, the response of fire season length to warming

408   was strongest for PFT-MC. Specifically, for PFT-MC, warming under RCP 8.5 led to an increase

409   of 21.6% (22 days) in fire season length (Fig. 5 b) and warming under RCP 4.5 led to an increase

410   of 10.8% (11 days) in fire season length. For PFT-LA, warming under RCP 8.5 led to an increase

411   of 14.7% (19 days) in fire season length (Fig. 5 a) while warming under RCP 4.5 led to an

412   increase of 7.4% (9 days) in fire season length. Finally, for PFT-HA, warming under RCP 8.5 led

413   to an increase of 10.2% (18 days) in fire season length (Fig. 5 c) and 5.3% (8 days) in fire season

414   length with under RCP 4.5. Because PFT-MC has a more conservative hydraulic strategy with

415   less negative P_{50}, turgor loss point and water potential at full turgor, this result supported

416   hypothesis H_4 that the LFMC for plants with more conservative hydraulic strategy will be more

417   vulnerable to warming.

418   To validate our classification scheme, we compared these PFT-level results to those

419   obtained with single-PFT and 2-PFT simulations finding that using the three PFTs defined by our

420   cluster analysis gives a qualitatively different view of LFMC change than a single- or 2-PFT

421   simulation. We found significant differences in the percentage changes of LFMC and fire season

422   length between future period (2080-2099) and historical period (1960-1999) using three distinct

423   PFTs, but no significant differences between PFTs in 2-PFT simulations under the different

424   climate scenarios (Fig. S6).

425   **4. Discussion**

426   Low LFMC within shrub leaves and shoots increases the flammability and likelihood of

427   combustion, making it vitally important to monitor temporal variations in LFMC, especially

428   during the dry season (Dennison et al, 2008). The strong relationships between observed and

429   simulated LFMC of all PFTs (Fig. 2) suggested that the plant hydrodynamic model, FATES-

430   HYDRO, could accurately estimate LFMC seasonal dynamics as a function of modeled leaf

431   water content, and consequently be useful to predict fire risks in Mediterranean-type climate

432   regions, although only small amount of validation data were used and the underlying assumption

433   that a shrub was analogous to a small tree. Based on the simulated monthly mean LFMC during

434   2006-2019 for PFT-LA, which includes the chamise species, we found that our model can

435   capture the seasonal variation and interannual variability, but underestimates the highest wet

436   season peaks in LFMC in 4 of 14 years (Fig. S5). This may cause biases for future projections

437   while it would not highly affect the long-term trend of LFMC and fire season length. During the

438   future period (2080-2099) and the historical period (1960-1999), both periods displayed lower

439   values in the dry season (April - October), which is consistent with lower LFMC during the

440   summer-fall dry season, rather than the winter-spring wet season (Chuvieco et al, 2004;

441   Pellizzaro et al, 2007; Pivovaroff et al. 2019). Extremely low daily LFMC was more likely to

442   occur during the future period, which had higher temperature than the historical period. From the

443   historical to the future period, fire season length could increase by 5.2-14.8% under climate

444   change for chaparral shrub ecosystems (H_0). The fire season length was not validated, rather it

445   was defined as number of days with LFMC below 79%.

446   Quantifying influences of climatic variables on LFMC is crucial to predicting future fire

447   risks (Dennison & Moritz, 2009). Our results showed that future warming was the most

448   important driver of LFMC. This finding suggested that warming would substantially push Vapor

449   Pressure Deficit (VPD) higher and decrease LFMC and strongly increase the fire season length,

450   which may greatly increase fire risks in the future (e.g. Dennison et al, 2008; Chuvieco et al,

451 2009; Pimont et al, 2019). CO_2 fertilization is expected to reduce stomatal conductance (Pataki et

452 al. 2000; Tognetti et al. 2000) and thus could mitigate the impacts of warming on LFMC. Our

453 results illustrated that, even though the CO_2 impact did cause a 3.5-4.8% reduction in fire season

454 length, the impact of warming on fire season length is about 5.6-13.8% larger than the CO_2 effect

455 (H_1, warming has a stronger impact on LFMC than CO_2 fertilization). This result suggests that

456 CO_2 fertilization cannot offset the LFMC impacts from warming. The FATES-HYDRO model

457 assumes a consistent stomatal sensitivity to CO_2 concentration across Mediterranean shrub

458 species. While Mediterranean shrub functional types in arid and semi-arid systems would vary in

459 their stomatal response in the real world (Pataki et al. 2000). Therefore, our model may

460 overestimate/underestimate the CO_2 effect on stomatal conductance and its mitigating influence

461 might be smaller in reality for some species.

462   Previous studies implied that the timing of precipitation may have a strong impact on

463 subsequent LFMC (e.g. Veblen et al. 2000; Westerling et al. 2006; Dennison & Moritz 2009). In

464 this study, precipitation was also a key driver of LFMC under future climate conditions. Our

465 results showed that, even though total precipitation was projected to increase, the reduction in

466 spring and autumn precipitation (Fig. S2) was projected to cause a longer fire season length (H_2,

467 the reductions in spring and autumn precipitation lead to a longer fire season as determined by

468 LFMC; Fig. 5). This result was in agreement with a prior study indicating that spring

469 precipitation, particularly in the month of March, was found to be the primary driver of timing of

470 LFMC changes (Dennison & Moritz 2009). We also found that the combined impacts of

471 warming and precipitation on fire season length were equal to the linearly additive impacts of

472 warming and precipitation change individually (H_3). Our results suggested that, when evaluating

473   future fire risks, it is critical that we considered the seasonal changes in precipitation and its

474   interaction with the warming impact.

475   Modeled vegetation responses to environmental changes is a function of variation in plant

476   functional traits (Koven et al, 2020). The three PFTs represented in this study have similar

477   patterns in LFMC in response to climate change during 1960-2099, but we did see some critical

478   differences. Specifically, the plant functional type PFT-MC with more conservative hydraulic

479   strategy had the strongest responses to climate change (Fig. 5). This could be related to the fact

480   that the PFT-MC is a more conservative drought tolerant PFT in terms of hydraulic strategy with

481   less negative P_{50}, turgor loss point, and water potential at full turgor. The PFT-MC plants had a

482   relatively high saturated water content based on observed data (Fig 2) and the water within plant

483   tissues thus changes more quickly in response to the environmental condition changes (H_4,

484   LFMC for plants with more conservative hydraulic strategies will be more vulnerable to

485   warming). However, the three different PFTs were coexisting at the same location in model

486   simulations, coexistence and heterogeneity in LFMC might impact fire behavior and fire season

487   length.

488   Because the moisture content of live fuels (~50–200%) are much higher than that of dead

489   fuels (~7–30%), leaf senescence induced by drought stress and subsequent mortality are

490   potentially vital factors to cause large wildfires (Nolan et al. 2016, 2020). Thus drought-induced

491   canopy die-back and mortality could largely increase surface fine fuel loads and vegetation

492   flammability, which can increase the probability of wildfire (Ruthrof et al. 2016). Since growth

493   and mortality are turned off in model runs by using a reduced-complexity configuration, it is

494   possible that vegetation density might decrease and LFMC could be conserved under future

495   scenarios. In addition, potential vegetation transitions (e.g., shrubs to grassland and species

496 composition changes) might substantially affect flammability and thus fire intensity and

497 frequency. In this study, we used the static mode of FATES-HYDRO to simulate LWC dynamics

498 under climate change. If we need to assess how the leaf senescence and vegetation dynamics will

499 impact the fire behavior, we can use the same model with dynamic mode to assess their impacts

500 on fire behaviors under future drought and warming conditions.

501 Application of a hydrodynamic vegetation model to estimate LFMC dynamics could

502 potentially benefit wildfire modeling at the fine-scale, landscape-scale, and global-scale. This is

503 because LFMC is one of the most critical factors influencing combustion, fire spread, and fire

504 consumption while previous wildfire models mainly focus on impacts of dead fuel moisture,

505 weather conditions on wildfire, fuel loads, and representation of live fuel moisture (Anderson &

506 Anderson 2010; Keeley et al. 2011; Jolly & Johnson 2018). The implications of this are that fire

507 potential will vary with plant water potential and uptake from soils, photosynthetic and

508 respiratory activity, carbon allocation and phenology with variability across species and over

509 time (Jolly & Johnson 2018). Therefore, future work to incorporate LFMC dynamics in wildfire

510 models could potentially play a vitally important role in the future studies of wildfire modeling

511 under climate change.

512 **5. Conclusions**

513 A hydrodynamic vegetation model, FATES-HYDRO, was used to estimate leaf water

514 status and thus LFMC dynamics of chaparral shrub species in southern California under

515 historical and future conditions. FATES-HYDRO model was validated using monthly mean

516 LFMC for three PFTs. The fire season length was projected to substantially increase under both

517 climate scenarios from 1960-1999 to 2080-2099. This could increase wildlife risk over time for

518 chaparral shrubs in southern California. Our results showed that temperature was the most

519   important driver of LFMC among all climatic variables. The LFMC estimated by the FATES-

520   HYDRO model offered a baseline of predicting plant hydraulic dynamics subjected to climate

521   change and provided a critical foundation that reductions in LFMC from climate warming may

522   exacerbate future wildfire risk. Longer fire season might have a significant impact on overall

523   public health and quality of life in the future.

524   **Acknowledgements**

525   This project is supported by the University of California Office of the President Lab Fees

526   Research Program and the Next Generation Ecosystem Experiment (NGEE) Tropics, which is

527   supported by the U.S. DOE Office of Science. CDK and JD are supported by the DOE Office of

528   Science, Regional and Global Model Analysis Program, Early Career Research Program. R

529   statistical software is applied to make figures for this study. A repository link for FATES is

530   https://github.com/xuchongang/fates.

531   **References**

532   Abatzoglou, J.T. and Brown, T.J., 2012. A comparison of statistical downscaling methods suited

533   for wildfire applications. *International Journal of Climatology*, *32*(5), pp.772-780.

534   Abatzoglou JT (2013) Development of gridded surface meteorological data for ecological

535   applications and modelling. *International Journal of Climatology*, 33, 121-131.Agee, J.K.,

536   Wright, C.S., Williamson, N. and Huff, M.H., 2002. Foliar moisture content of Pacific Northwest

537   vegetation and its relation to wildland fire behavior. *Forest ecology and management*, *167*(1-3),

538   pp.57-66.

539   Anderson, S.A. and Anderson, W.R., 2010. Ignition and fire spread thresholds in gorse (Ulex

540   europaeus). *International Journal of Wildland Fire*, *19*(5), pp.589-598.

541   Aguado, I., Chuvieco, E., Boren, R. and Nieto, H., 2007. Estimation of dead fuel moisture

542   content from meteorological data in Mediterranean areas. Applications in fire danger assessment.

543   *International Journal of Wildland Fire*, *16*(4), pp.390-397.

544   Bistinas, I., Harrison, S.P., Prentice, I.C. and Pereira, J.M.C., 2014. Causal relationships versus

545   emergent patterns in the global controls of fire frequency. *Biogeosciences*, *11*(18), pp.5087-5101.

546   Burgan, R.E. Estimating Live Fuel Moisture for the 1978 National Fire Danger Rating System;

547   Intermountain Forest and Range Experiment Station: Ogden, UT, USA, 1979.

548   Bilgili, E. and Saglam, B., 2003. Fire behavior in maquis fuels in Turkey. *Forest Ecology and*

549   *Management*, *184*(1-3), pp.201-207.

550   Balch, J.K., Bradley, B.A., Abatzoglou, J.T., Nagy, R.C., Fusco, E.J. and Mahood, A.L., 2017.

551   Human-started wildfires expand the fire niche across the United States. *Proceedings of the*

552   *National Academy of Sciences*, *114*(11), pp.2946-2951.

553   Bartlett, M.K., Scoffoni, C. and Sack, L., 2012. The determinants of leaf turgor loss point and

554   prediction of drought tolerance of species and biomes: a global meta-analysis. *Ecology letters*,

555   *15*(5), pp.393-405.

556   Bridges Jr, C.C., 1966. Hierarchical cluster analysis. *Psychological reports*, *18*(3), pp.851-854.

557   Christoffersen, B.O., Gloor, M., Fauset, S., Fyllas, N.M., Galbraith, D.R., Baker, T.R., Kruijt, B.,

558   Rowland, L., Fisher, R.A., Binks, O.J. and Sevanto, S., 2016. Linking hydraulic traits to tropical

559   forest function in a size-structured and trait-driven model (TFS v. 1-Hydro). Geoscientific Model

560   Development. 9: 4227-4255.

561 Caccamo, G., Chisholm, L.A., Bradstock, R.A. and Puotinen, M.L., 2012a. Using remotely-

562 sensed fuel connectivity patterns as a tool for fire danger monitoring. *Geophysical Research*

563 *Letters*, *39*(1).

564 Caccamo, G., Chisholm, L.A., Bradstock, R.A., Puotinen, M.L. and Pippen, B.G., 2012b.

565 Monitoring live fuel moisture content of heathland, shrubland and sclerophyll forest in south-

566 eastern Australia using MODIS data. *International Journal of Wildland Fire*, *21*(3), pp.257-269.

567 Clarke, H., Pitman, A.J., Kala, J., Carouge, C., Haverd, V. and Evans, J.P., 2016. An

568 investigation of future fuel load and fire weather in Australia. *Climatic Change*, *139*(3-4),

569 pp.591-605.

570 Chuvieco, E., Cocero, D., Riano, D., Martin, P., Martınez-Vega, J., de la Riva, J. and Pérez, F.,

571 2004. Combining NDVI and surface temperature for the estimation of live fuel moisture content

572 in forest fire danger rating. Remote Sensing of Environment, 92(3), pp.322-331.

573 Caldwell, P.M., Mametjanov, A., Tang, Q., Van Roekel, L.P., Golaz, J.C., Lin, W., Bader, D.C.,

574 Keen, N.D., Feng, Y., Jacob, R. and Maltrud, M.E., 2019. The DOE E3SM coupled model

575 version 1: Description and results at high resolution. *Journal of Advances in Modeling Earth*

576 *Systems*, *11*(12), pp.4095-4146.

577 Castro, F.X., Tudela, A. and Sebastià, M.T., 2003. Modeling moisture content in shrubs to

578 predict fire risk in Catalonia (Spain). *Agricultural and Forest Meteorology*, *116*(1-2), pp.49-59.

579 Chuvieco, E., González, I., Verdú, F., Aguado, I. and Yebra, M., 2009. Prediction of fire

580 occurrence from live fuel moisture content measurements in a Mediterranean ecosystem.

581 *International Journal of Wildland Fire*, *18*(4), pp.430-441.

582   Collins, M., Knutti, R., Arblaster, J., Dufresne, J.L., Fichefet, T., Friedlingstein, P., Gao, X.,

583   Gutowski, W.J., Johns, T., Krinner, G. and Shongwe, M., 2013. Long-term climate change:

584   projections, commitments and irreversibility. In *Climate Change 2013-The Physical Science*

585   *Basis: Contribution of Working Group I to the Fifth Assessment Report of the Intergovernmental*

586   *Panel on Climate Change* (pp. 1029-1136). Cambridge University Press.

587   Cook, B.I., Smerdon, J.E., Seager, R. and Coats, S., 2014. Global warming and 21 st century

588   drying. *Climate Dynamics*, *43*(9-10), pp.2607-2627.

589   Dennison, P.E., Moritz, M.A. and Taylor, R.S., 2008. Evaluating predictive models of critical

590   live fuel moisture in the Santa Monica Mountains, California. *International Journal of Wildland*

591   *Fire*, *17*(1), pp.18-27.

592   Dennison, P.E. and Moritz, M.A., 2009. Critical live fuel moisture in chaparral ecosystems: a

593   threshold for fire activity and its relationship to antecedent precipitation. *International Journal of*

594   *Wildland Fire*, *18*(8), pp.1021-1027.

595   Dimitrakopoulos, A.P. and Papaioannou, K.K., 2001. Flammability assessment of Mediterranean

596   forest fuels. *Fire Technology*, *37*(2), pp.143-152.

597   Dai, A., 2013. Increasing drought under global warming in observations and models. *Nature*

598   *climate change*, *3*(1), pp.52-58.

599   Duursma, R.A. and Medlyn, B.E., 2012. MAESPA: a model to study interactions between water

600   limitation, environmental drivers and vegetation function at tree and stand levels, with an

601   example application to [CO_2]×drought interactions.

602 Flannigan, M.D., Krawchuk, M.A., de Groot, W.J., Wotton, B.M. and Gowman, L.M., 2009.

603 Implications of changing climate for global wildland fire. *International journal of wildland fire*,

604 *18*(5), pp.483-507.

605 Fisher, R.A., Williams, M., Da Costa, A.L., Malhi, Y., Da Costa, R.F., Almeida, S. and Meir, P.,

606 2007. The response of an Eastern Amazonian rain forest to drought stress: results and modelling

607 analyses from a throughfall exclusion experiment. *Global Change Biology*, *13*(11), pp.2361-

608 2378.

609 Fisher, R.A., Muszala, S., Verteinstein, M., Lawrence, P., Xu, C., McDowell, N.G., Knox, R.G.,

610 Koven, C., Holm, J., Rogers, B.M. and Spessa, A., 2015. Taking off the training wheels: the

611 properties of a dynamic vegetation model without climate envelopes, CLM4. 5 (ED).

612 *Geoscientific Model Development*, *8*(11), pp.3593-3619.

613 Fisher, R.A., Koven, C.D., Anderegg, W.R., Christoffersen, B.O., Dietze, M.C., Farrior, C.E.,

614 Holm, J.A., Hurtt, G.C., Knox, R.G., Lawrence, P.J. and Lichstein, J.W., 2018. Vegetation

615 demographics in Earth System Models: A review of progress and priorities. *Global change

616 biology*, *24*(1), pp.35-54.

617 Gillett, N.P., Weaver, A.J., Zwiers, F.W. and Flannigan, M.D., 2004. Detecting the effect of

618 climate change on Canadian forest fires. *Geophysical Research Letters*, *31*(18).

619 Goss, M., Swain, D.L., Abatzoglou, J.T., Sarhadi, A., Kolden, C.A., Williams, A.P. and

620 Diffenbaugh, N.S., 2020. Climate change is increasing the likelihood of extreme autumn wildfire

621 conditions across California. *Environmental Research Letters*, *15*(9), p.094016.

622 Hantson, S., Arneth, A., Harrison, S.P., Kelley, D.I., Prentice, I.C., Rabin, S.S., Archibald, S.,

623 Mouillot, F., Arnold, S.R., Artaxo, P. and Bachelet, D., 2016. The status and challenge of global

624 fire modelling. *Biogeosciences*, *13*(11), pp.3359-3375.

625 Holm, J.A., Shugart, H.H., Van Bloem, S.J. and Larocque, G.R., 2012. Gap model development,

626 validation, and application to succession of secondary subtropical dry forests of Puerto Rico.

627 *Ecological Modelling*, *233*, pp.70-82.

628 Jacobsen, A. L., Pratt, R. B., Davis, S. D., & Ewers, F. W. (2008). Comparative community

629 physiology: nonconvergence in water relations among three semi-arid shrub communities. New

630 Phytologist, 180(1), 100-113.

631 Jolly, W.M. and Johnson, D.M., 2018. Pyro-ecophysiology: shifting the paradigm of live

632 wildland fuel research. *Fire*, *1*(1), p.8.

633 Jackson, D.A., 1993. Stopping rules in principal components analysis: a comparison of

634 heuristical and statistical approaches. *Ecology*, *74*(8), pp.2204-2214.

635 Kelley, D.I., Bistinas, I., Whitley, R., Burton, C., Marthews, T.R. and Dong, N., 2019. How

636 contemporary bioclimatic and human controls change global fire regimes. *Nature Climate*

637 *Change*, *9*(9), pp.690-696.

638 Konings, A.G., Rao, K. and Steele-Dunne, S.C., 2019. Macro to micro: microwave remote

639 sensing of plant water content for physiology and ecology. *New Phytologist*, *223*(3), pp.1166-

640 1172.

641 Keeley, J.E., 1995. Future of California floristics and systematics: wildfire threats to the

642 California flora. Madrono, pp.175-179.

643 Keeley, J.E. and Zedler, P.H., 2009. Large, high-intensity fire events in southern California

644 shrublands: debunking the fine-grain age patch model. *Ecological Applications*, *19*(1), pp.69-94.

645 Keeley, J.E., Bond, W.J., Bradstock, R.A., Pausas, J.G. and Rundel, P.W., 2011. *Fire in*

646 *Mediterranean ecosystems: ecology, evolution and management*. Cambridge University Press.

647 Kennedy, D., Swenson, S., Oleson, K.W., Lawrence, D.M., Fisher, R., Lola da Costa, A.C. and

648 Gentine, P., 2019. Implementing plant hydraulics in the community land model, version 5.

649 *Journal of Advances in Modeling Earth Systems*, *11*(2), pp.485-513.

650 Koven, C.D., Knox, R.G., Fisher, R.A., Chambers, J.Q., Christoffersen, B.O., Davies, S.J.,

651 Detto, M., Dietze, M.C., Faybishenko, B., Holm, J. and Huang, M., 2020. Benchmarking and

652 parameter sensitivity of physiological and vegetation dynamics using the Functionally

653 Assembled Terrestrial Ecosystem Simulator (FATES) at Barro Colorado Island, Panama.

654 *Biogeosciences*, *17*(11), pp.3017-3044.

655 Krawchuk, M.A., Moritz, M.A., Parisien, M.A., Van Dorn, J. and Hayhoe, K., 2009. Global

656 pyrogeography: the current and future distribution of wildfire. *PloS one*, *4*(4), p.e5102.Linn, R.,

657 Reisner, J., Colman, J.J. and Winterkamp, J., 2002. Studying wildfire behavior using FIRETEC.

658 *International journal of wildland fire*, *11*(4), pp.233-246.

659 Liu, Y., Stanturf, J. and Goodrick, S., 2010. Trends in global wildfire potential in a changing

660 climate. *Forest ecology and management*, *259*(4), pp.685-697.

661 Massoud, E.C., Xu, C., Fisher, R.A., Knox, R.G., Walker, A.P., Serbin, S.P., Christoffersen,

662 B.O., Holm, J.A., Kueppers, L.M., Ricciuto, D.M. and Wei, L., 2019. Identification of key

663 parameters controlling demographically structured vegetation dynamics in a land surface model:

664 CLM4. 5 (FATES). *Geoscientific Model Development*, *12*(9), pp.4133-4164.

665   Moorcroft, P.R., Hurtt, G.C. and Pacala, S.W., 2001. A method for scaling vegetation dynamics:

666   the ecosystem demography model (ED). *Ecological monographs*, *71*(4), pp.557-586.

667   Mikkelsen, T.N., Beier, C., Jonasson, S., Holmstrup, M., Schmidt, I.K., Ambus, P., Pilegaard,

668   K., Michelsen, A., Albert, K., Andresen, L.C. and Arndal, M.F., 2008. Experimental design of

669   multifactor climate change experiments with elevated CO2, warming and drought: the

670   CLIMAITE project. *Functional Ecology*, *22*(1), pp.185-195.

671   Moritz, M.A., Parisien, M.A., Batllori, E., Krawchuk, M.A., Van Dorn, J., Ganz, D.J. and

672   Hayhoe, K., 2012. Climate change and disruptions to global fire activity. *Ecosphere*, *3*(6), pp.1-

673   22.

674   McDowell, N.G., Fisher, R.A., Xu, C., Domec, J.C., Hölttä, T., Mackay, D.S., Sperry, J.S.,

675   Boutz, A., Dickman, L., Gehres, N. and Limousin, J.M., 2013. Evaluating theories of drought-

676   induced vegetation mortality using a multimodel–experiment framework. *New Phytologist*,

677   *200*(2), pp.304-321.

678   Mencuccini, M., Manzoni, S. and Christoffersen, B., 2019. Modelling water fluxes in plants:

679   from tissues to biosphere. *New Phytologist*, *222*(3), pp.1207-1222.

680   Matthews, S., Sullivan, A.L., Watson, P. and Williams, R.J., 2012. Climate change, fuel and fire

681   behaviour in a eucalypt forest. *Global Change Biology*, *18*(10), pp.3212-3223.

682   Manabe, S. and Wetherald, R.T., 1975. The effects of doubling the CO2 concentration on the

683   climate of a general circulation model. *Journal of the Atmospheric Sciences*, *32*(1), pp.3-15.

684   Meinzer, F.C., James, S.A., Goldstein, G. and Woodruff, D., 2003. Whole-tree water transport

685   scales with sapwood capacitance in tropical forest canopy trees. *Plant, Cell & Environment*,

686   *26*(7), pp.1147-1155.

687   Meinzer, F.C., Johnson, D.M., Lachenbruch, B., McCulloh, K.A. and Woodruff, D.R., 2009.

688   Xylem hydraulic safety margins in woody plants: coordination of stomatal control of xylem

689   tension with hydraulic capacitance. *Functional Ecology*, *23*(5), pp.922-930.

690   Meinshausen, M., Smith, S.J., Calvin, K., Daniel, J.S., Kainuma, M.L., Lamarque, J.F.,

691   Matsumoto, K., Montzka, S.A., Raper, S.C., Riahi, K. and Thomson, A.G.J.M.V., 2011. The

692   RCP greenhouse gas concentrations and their extensions from 1765 to 2300. *Climatic change*,

693   *109*(1), pp.213-241.

694   Nolan, R.H., Boer, M.M., Resco de Dios, V., Caccamo, G. and Bradstock, R.A., 2016. Large-

695   scale, dynamic transformations in fuel moisture drive wildfire activity across southeastern

696   Australia. *Geophysical Research Letters*, *43*(9), pp.4229-4238.

697   Nolan, R.H., Blackman, C.J., de Dios, V.R., Choat, B., Medlyn, B.E., Li, X., Bradstock, R.A.

698   and Boer, M.M., 2020. Linking forest flammability and plant vulnerability to drought. *Forests*,

699   *11*(7), p.779.

700   National Fuel Moisture Database. 2021.

701   https://www.wfas.net/nfmd/public/site.php?site_fuel=Stunt%20Road%2C%20Calabasas&gacc=

702   SOCC&state=CA&grup=LA%20County&sitefuel=site&display_type=Table%20Only%20Actua

703   l%20Data&fuel_selected=Chamise.

704   Pivovaroff, A. L., Emery, N., Sharifi, M. R., Witter, M., Keeley, J. E., & Rundel, P. W. (2019).

705   The effect of ecophysiological traits on live fuel moisture content. Fire, 2(2), 28.

706 Powell, T.L., Koven, C.D., Johnson, D.J., Faybishenko, B., Fisher, R.A., Knox, R.G., McDowell,

707 N.G., Condit, R., Hubbell, S.P., Wright, S.J. and Chambers, J.Q., 2018. Variation in

708 hydroclimate sustains tropical forest biomass and promotes functional diversity. *New*

709 *Phytologist*, *219*(3), pp.932-946.

710 Pellizzaro, G., Cesaraccio, C., Duce, P., Ventura, A. and Zara, P., 2007. Relationships between

711 seasonal patterns of live fuel moisture and meteorological drought indices for Mediterranean

712 shrubland species. *International Journal of Wildland Fire*, *16*(2), pp.232-241.

713 Plucinski, M.P., 2003. The investigation of factors governing ignition and development of fires

714 in heathland vegetation. *PhD thesis. University of New South Wales, Sydney.*

715 Pimont, F., Ruffault, J., Martin-StPaul, N.K. and Dupuy, J.L., 2019. Why is the effect of live fuel

716 moisture content on fire rate of spread underestimated in field experiments in shrublands?.

717 *International journal of wildland fire*, *28*(2), pp.127-137.

718 Pataki, D.E., Huxman, T.E., Jordan, D.N., Zitzer, S.F., Coleman, J.S., Smith, S.D., Nowak, R.S.

719 and Seemann, J.R., 2000. Water use of two Mojave Desert shrubs under elevated CO2. *Global*

720 *Change Biology*, *6*(8), pp.889-897.

721 Pineda-Garcia, F., Paz, H. and Meinzer, F.C., 2013. Drought resistance in early and late

722 secondary successional species from a tropical dry forest: the interplay between xylem resistance

723 to embolism, sapwood water storage and leaf shedding. *Plant, Cell & Environment*, *36*(2),

724 pp.405-418.

725 Rabin, S.S., Melton, J.R., Lasslop, G., Bachelet, D., Forrest, M., Hantson, S., Kaplan, J.O., Li,

726 F., Mangeon, S., Ward, D.S. and Yue, C., 2017. The Fire Modeling Intercomparison Project

727 (FireMIP), phase 1: experimental and analytical protocols with detailed model descriptions.

728 *Geoscientific Model Development*, *10*(3), pp.1175-1197.

729 Rossa, C.G. and Fernandes, P.M., 2018. Live fuel moisture content: The 'pea under the mattress'

730 of fire spread rate modeling?. *Fire*, *1*(3), p.43.

731 Rind, D., Goldberg, R., Hansen, J., Rosenzweig, C. and Ruedy, R., 1990. Potential

732 evapotranspiration and the likelihood of future drought. *Journal of Geophysical Research:*

733 *Atmospheres*, *95*(D7), pp.9983-10004.

734 Rothermel, R.C., 1972. *A mathematical model for predicting fire spread in wildland fuels* (Vol.

735 115). Intermountain Forest & Range Experiment Station, Forest Service, US Department of

736 Agriculture.

737 Ruthrof, K.X., Fontaine, J.B., Matusick, G., Breshears, D.D., Law, D.J., Powell, S. and Hardy,

738 G., 2016. How drought-induced forest die-off alters microclimate and increases fuel loadings and

739 fire potentials. *International Journal of Wildland Fire*, *25*(8), pp.819-830.

740 Sturtevant, B.R., Scheller, R.M., Miranda, B.R., Shinneman, D. and Syphard, A., 2009.

741 Simulating dynamic and mixed-severity fire regimes: a process-based fire extension for

742 LANDIS-II. *Ecological Modelling*, *220*(23), pp.3380-3393.

743 Stocks, B.J., Fosberg, M.A., Lynham, T.J., Mearns, L., Wotton, B.M., Yang, Q., Jin, J.Z.,

744 Lawrence, K., Hartley, G.R., Mason, J.A. and McKenney, D.W., 1998. Climate change and

745 forest fire potential in Russian and Canadian boreal forests. *Climatic change*, *38*(1), pp.1-13.

746   Schroeder, M.J., Glovinsky, M., Henricks, V.F., Hood, F.C. and Hull, M.K., 1964. *Synoptic*

747   *weather types associated with critical fire weather*. USDA Forest Service, Pacific Southwest

748   Range and Experiment Station. Berkeley, CA.

749   Seiler, C., Hutjes, R.W.A., Kruijt, B., Quispe, J., Añez, S., Arora, V.K., Melton, J.R., Hickler, T.

750   and Kabat, P., 2014. Modeling forest dynamics along climate gradients in Bolivia. *Journal of*

751   *Geophysical Research: Biogeosciences*, *119*(5), pp.758-775.

752   Sheffield, J. and Wood, E.F., 2008. Projected changes in drought occurrence under future global

753   warming from multi-model, multi-scenario, IPCC AR4 simulations. *Climate dynamics*, *31*(1),

754   pp.79-105.

755   Saura-Mas, S. and Lloret, F., 2007. Leaf and shoot water content and leaf dry matter content of

756   Mediterranean woody species with different post-fire regenerative strategies. *Annals of Botany*,

757   *99*(3), pp.545-554.

758   Sun, W., Maseyk, K., Lett, C. and Seibt, U., 2016. Litter dominates surface fluxes of carbonyl

759   sulfide in a Californian oak woodland. *Journal of Geophysical Research: Biogeosciences*,

760   *121*(2), pp.438-450.

761   Thonicke, K., Spessa, A., Prentice, I.C., Harrison, S.P., Dong, L. and Carmona-Moreno, C.,

762   2010. The influence of vegetation, fire spread and fire behaviour on biomass burning and trace

763   gas emissions: results from a process-based model. *Biogeosciences*, *7*(6), pp.1991-2011.

764   Tyree, M.T. and Hammel, H.T., 1972. The measurement of the turgor pressure and the water

765   relations of plants by the pressure-bomb technique. *Journal of experimental Botany*, *23*(1),

766   pp.267-282.

767   Tyree, M.T. and Yang, S., 1990. Water-storage capacity of Thuja, Tsuga and Acer stems

768   measured by dehydration isotherms. *Planta*, *182*(3), pp.420-426.

769   Tognetti, R., Minnocci, A., Peñuelas, J., Raschi, A. and Jones, M.B., 2000. Comparative field

770   water relations of three Mediterranean shrub species co-occurring at a natural CO2 vent. *Journal*

771   *of Experimental Botany*, *51*(347), pp.1135-1146.

772   Tjiputra, J.F., Roelandt, C., Bentsen, M., Lawrence, D.M., Lorentzen, T., Schwinger, J., Seland,

773   Ø. and Heinze, C., 2013. Evaluation of the carbon cycle components in the Norwegian Earth

774   System Model (NorESM). *Geoscientific Model Development*, *6*(2), pp.301-325.

775   Venturas, M. D., MacKinnon, E. D., Dario, H. L., Jacobsen, A. L., Pratt, R. B., & Davis, S. D.

776   (2016). Chaparral shrub hydraulic traits, size, and life history types relate to species mortality

777   during California's historic drought of 2014. PLOS One, 11(7).

778   Veblen, T.T., Kitzberger, T. and Donnegan, J., 2000. Climatic and human influences on fire

779   regimes in ponderosa pine forests in the Colorado Front Range. *Ecological applications*, *10*(4),

780   pp.1178-1195.

781   Westerling, A.L., Gershunov, A., Brown, T.J., Cayan, D.R. and Dettinger, M.D., 2003. Climate

782   and wildfire in the western United States. *Bulletin of the American Meteorological Society*,

783   *84*(5), pp.595-604.

784   Westerling, A.L., Hidalgo, H.G., Cayan, D.R. and Swetnam, T.W., 2006. Warming and earlier

785   spring increase western US forest wildfire activity. *science*, *313*(5789), pp.940-943.

786   Williams, A.P., Abatzoglou, J.T., Gershunov, A., Guzman-Morales, J., Bishop, D.A., Balch, J.K.

787   and Lettenmaier, D.P., 2019. Observed impacts of anthropogenic climate change on wildfire in

788   California. *Earth's Future*, *7*(8), pp.892-910.

789   Wullschleger, S.D., Gunderson, C.A., Hanson, P.J., Wilson, K.B. and Norby, R.J., 2002.

790   Sensitivity of stomatal and canopy conductance to elevated CO_2 concentration–interacting

791   variables and perspectives of scale. *New Phytologist*, *153*(3), pp.485-496.

792   Wu, J., Serbin, S.P., Ely, K.S., Wolfe, B.T., Dickman, L.T., Grossiord, C., Michaletz, S.T.,

793   Collins, A.D., Detto, M., McDowell, N.G. and Wright, S.J., 2020. The response of stomatal

794   conductance to seasonal drought in tropical forests. *Global Change Biology*, *26*(2), pp.823-839.

795   Wei, L., Xu, C., Jansen, S., Zhou, H., Christoffersen, B.O., Pockman, W.T., Middleton, R.S.,

796   Marshall, J.D. and McDowell, N.G., 2019. A heuristic classification of woody plants based on

797   contrasting shade and drought strategies. *Tree physiology*, *39*(5), pp.767-781.

798   Xu, C., McDowell, N.G., Sevanto, S. and Fisher, R.A., 2013. Our limited ability to predict

799   vegetation dynamics under water stress. *New Phytologist*, *200*(2), pp.298-300.

800   Xu, X., Medvigy, D., Powers, J.S., Becknell, J.M. and Guan, K., 2016. Diversity in plant

801   hydraulic traits explains seasonal and inter-annual variations of vegetation dynamics in

802   seasonally dry tropical forests. *New Phytologist*, *212*(1), pp.80-95.

803   Xu, C., McDowell, N.G., Fisher, R.A., Wei, L., Sevanto, S., Christoffersen, B.O., Weng, E. and

804   Middleton, R.S., 2019. Increasing impacts of extreme droughts on vegetation productivity under

805   climate change. *Nature Climate Change*, *9*(12), pp.948-953.

806   Yebra, M., Chuvieco, E. and Riaño, D., 2008. Estimation of live fuel moisture content from

807   MODIS images for fire risk assessment. *Agricultural and forest meteorology*, *148*(4), pp.523-

808   536.

809   Yebra, M., Dennison, P.E., Chuvieco, E., Riano, D., Zylstra, P., Hunt Jr, E.R., Danson, F.M., Qi,

810   Y. and Jurdao, S., 2013. A global review of remote sensing of live fuel moisture content for fire

811   danger assessment: Moving towards operational products. *Remote Sensing of Environment*, *136*,

812   pp.455-468.

813   Yebra, M., Quan, X., Riaño, D., Larraondo, P.R., van Dijk, A.I. and Cary, G.J., 2018. A fuel

814   moisture content and flammability monitoring methodology for continental Australia based on

815   optical remote sensing. *Remote Sensing of Environment*, *212*, pp.260-272.

816   Zarco-Tejada, P.J., Rueda, C.A. and Ustin, S.L., 2003. Water content estimation in vegetation

817   with MODIS reflectance data and model inversion methods. *Remote Sensing of Environment*,

818   *85*(1), pp.109-124.

819   Zhao, T. and Dai, A., 2015. The magnitude and causes of global drought changes in the twenty-

820   first century under a low–moderate emissions scenario. *Journal of climate*, *28*(11), pp.4490-

821   4512.

822

823
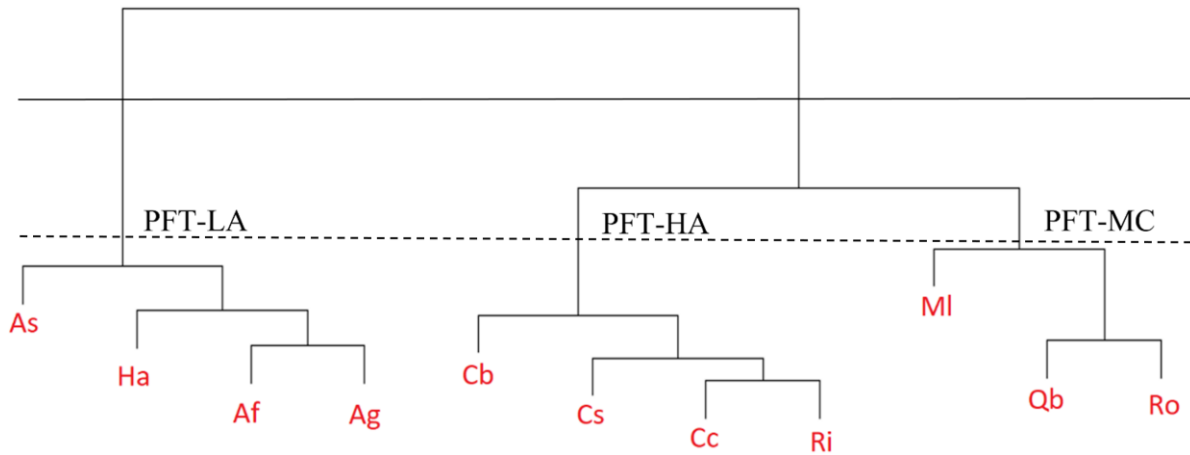
Fig 1. Hierarchical cluster analysis of allometry and hydraulic traits for eleven chaparral shrub species used to define three plant functional types at Stunt Ranch. The plant functional types with a low productivity and an aggressive drought tolerance hydraulic strategy (PFT-LA) was defined based on traits of red shank (Adenostoma sparsifolium - As), toyon (Heteromeles arbutifolia - Ha), chamise (Adenostoma fasciculatum - Af), big berry manzanita (Arctostaphylos glauca - Ag); the plant functional types with a high productivity and an aggressive drought tolerance hydraulic strategy (PFT-HA) was defined based on traits of mountain mahogany (Cercocarpus betuloides - Cb), greenbark ceanothus (Ceanothus spinosus - Cs), buck brush (Ceanothus cuneatus - Cc), hollyleaf redberry (Rhamnus ilicifolia - Ri); the plant functional types with a medium productivity and an conservative drought tolerance hydraulic strategy (PFT-MC) was defined based on traits of laurel sumac (Malosma laurina - Ml), scrub oak (Quercus berberidifolia - Qb), sugar bush (Rhus ovata - Ro).

836

837
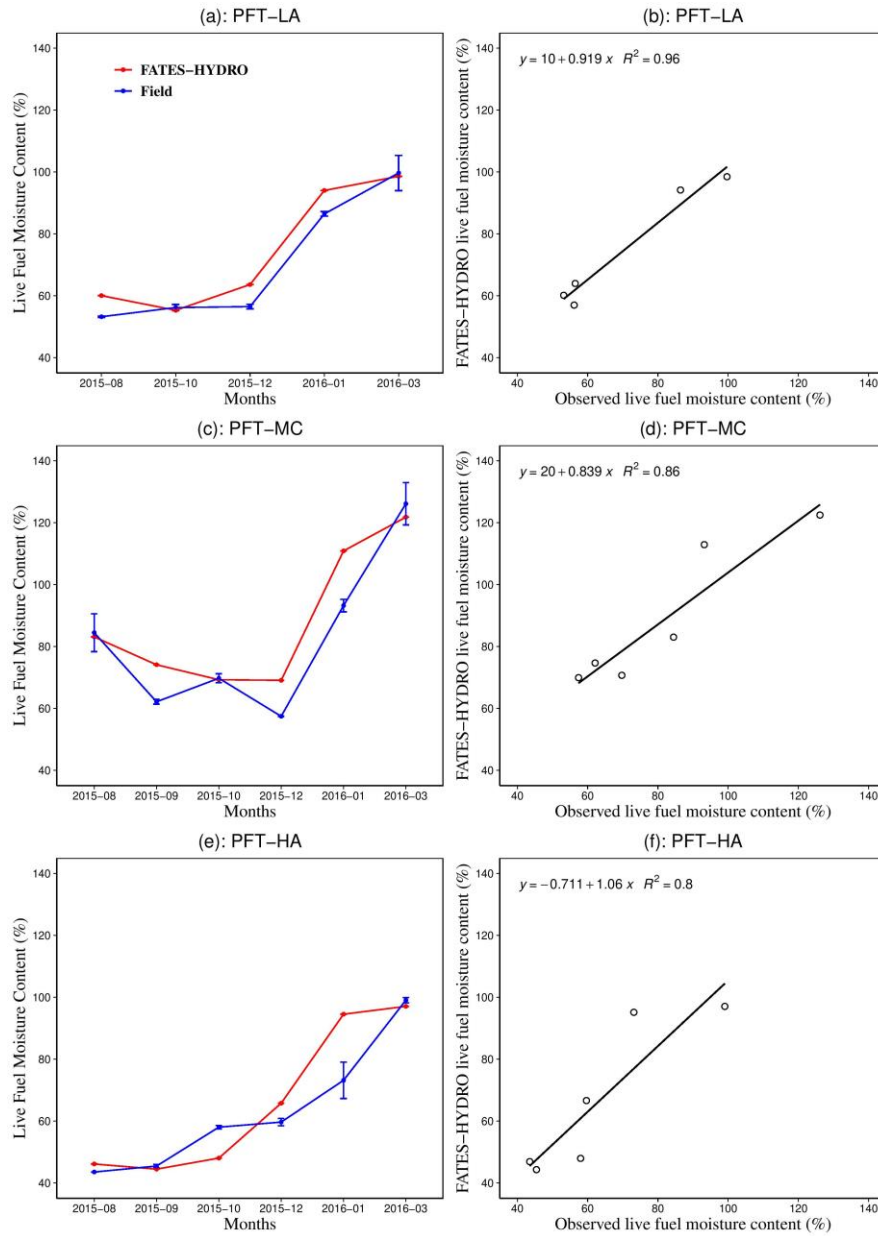
Fig.2 Simulated and observed monthly live fuel moisture content and related R^2 values for three PFTs (refer to Figure 1 for explanation of the PFTs).

840
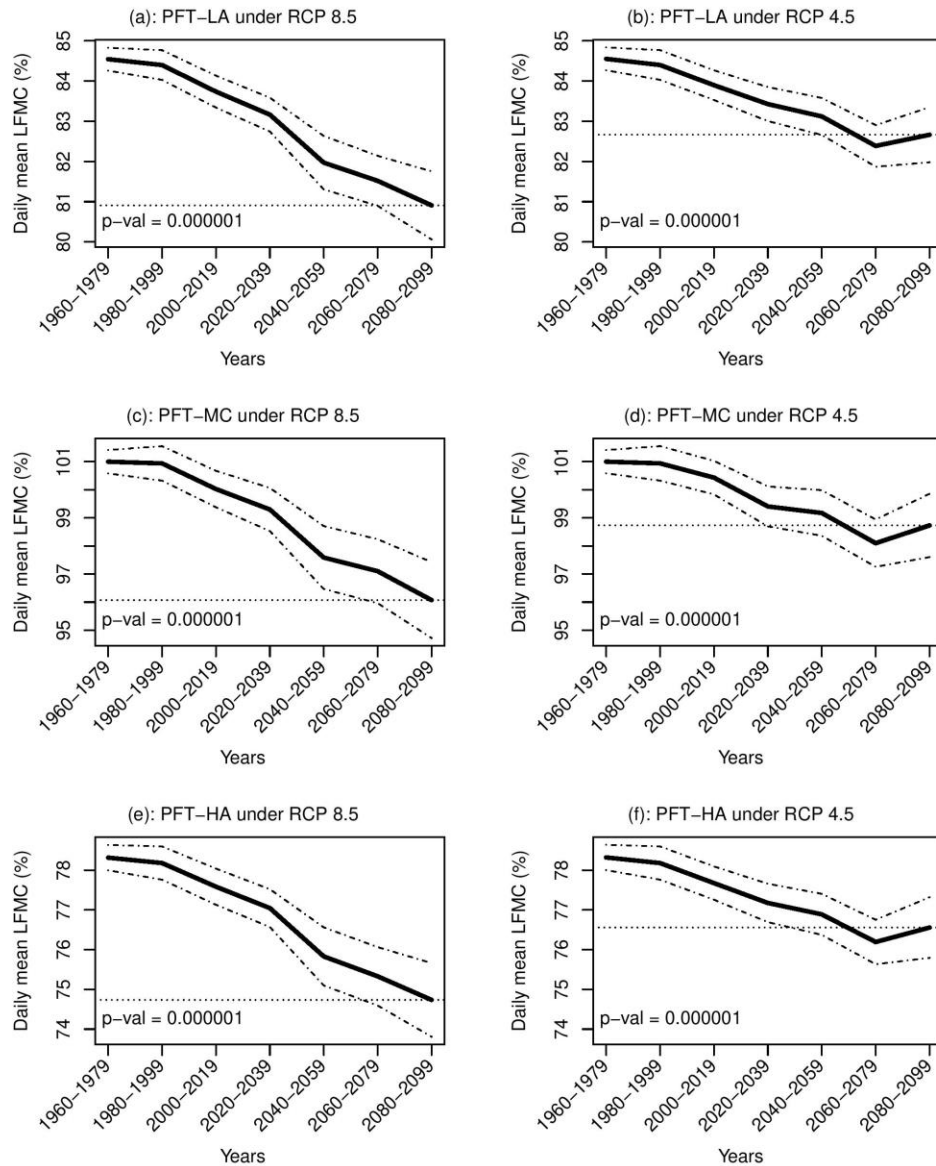
Fig.3 Temporal changes in daily mean live fuel moisture content (black solid line) and 95% confidence interval (black dash-dot line) from 1960 to 2099 for three PFTs (refer to Figure 1 for explanation of the PFTs) under climate scenario RCP 4.5 and 8.5 with 20 Earth System Models considering all climatic variables changes. The P values were calculated using bootstrap sampling to test whether the daily mean live fuel moisture content across different models during the future period (2080–2099) was significantly lower than that during the historical period (1960-1999). The grey horizontal dotted line represents the ensemble mean for 2080–2099.

848
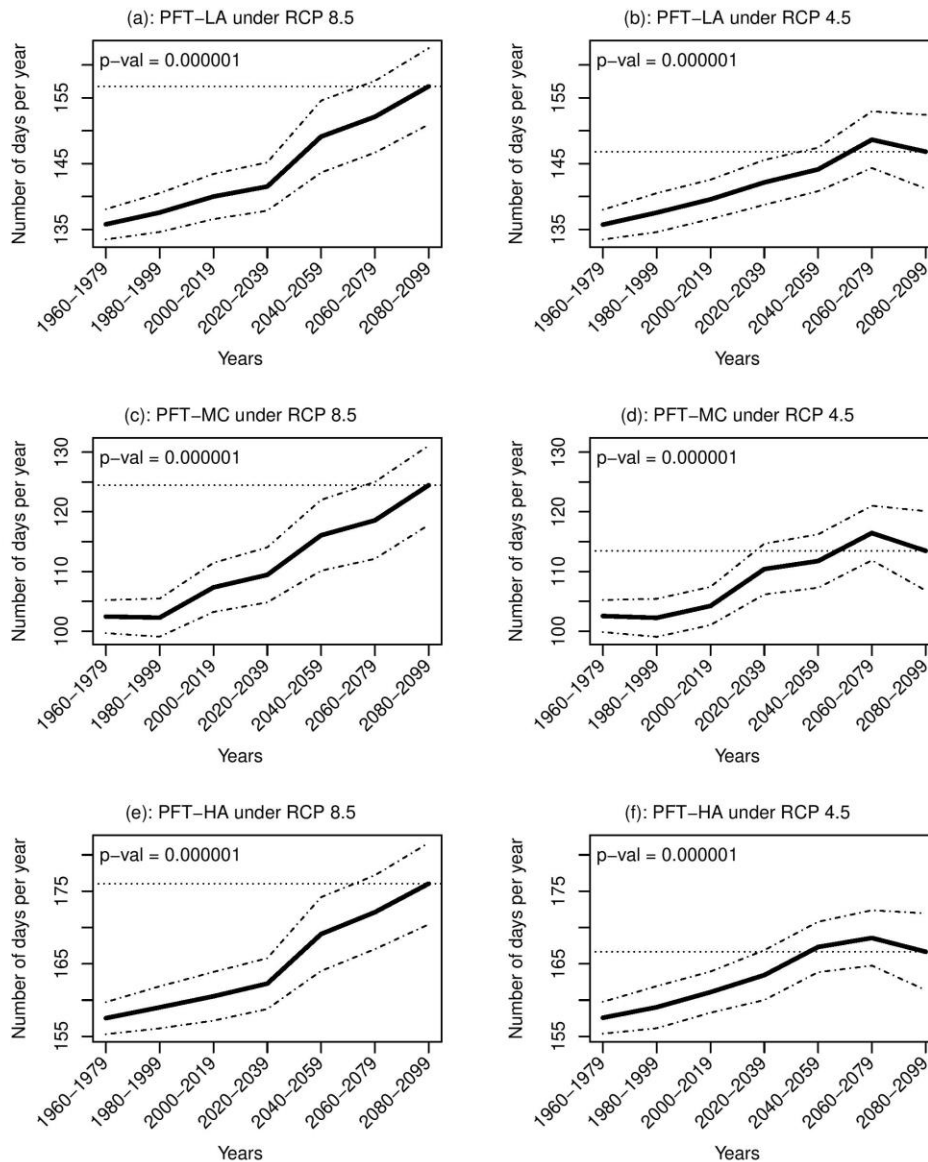
Fig.4 Temporal changes in average number of days per year of live fuel moisture content below 79% (black solid line) and 95% confidence interval (black dash-dot line) from 1960 to 2099 for three PFTs (refer to Figure 1 for explanation of the PFTs) under climate scenario RCP 4.5 and 8.5 with 20 Earth System Models considering all climatic variables changes. The P values were calculated using bootstrap sampling to test whether the number of days across different models during the future period (2080–2099) was significantly higher than that during the historical period (1960-1999). The grey horizontal dotted line represents the ensemble mean for 2080–2099.

857

858
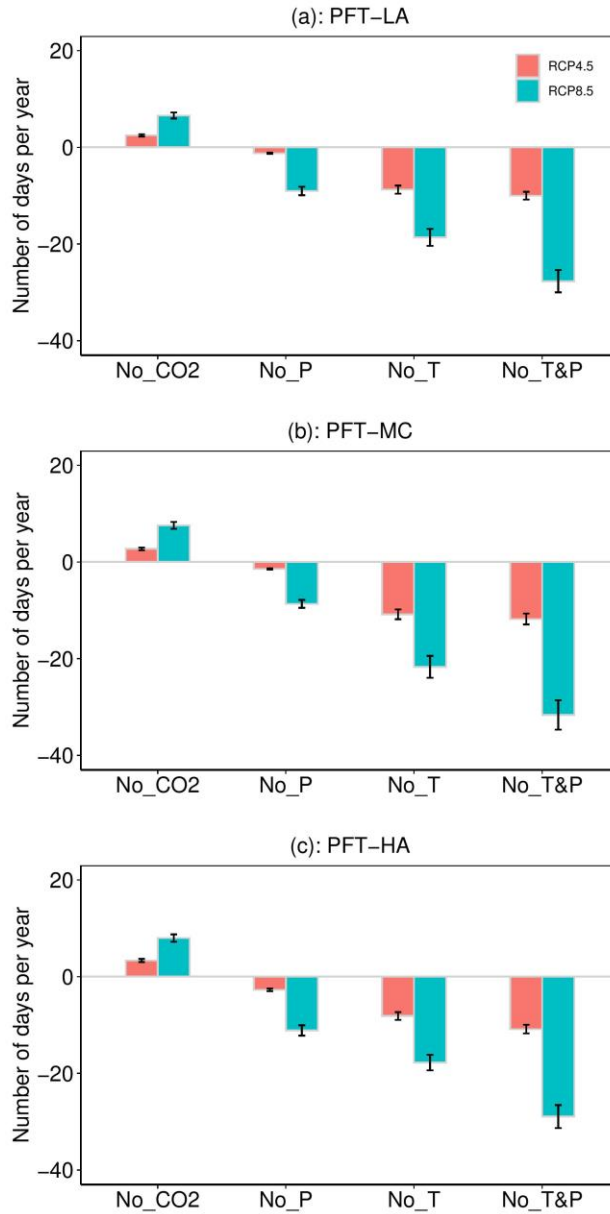
859

860 **Fig.5** Differences on number of days per year of live fuel moisture content below 79% from
861 2080 to 2099 for three PFTs (refer to Figure 1 for explanation of the PFTs) under climate
862 scenario RCP 4.5 and 8.5 between considering all climatic variables changes and without
863 considering CO_2, precipitation, temperature, and precipitation & temperature changes.